8488 *Biochemistry* **2010,** *49,* 8488–8498
DOI: 10.1021/bi100673c

BIOCHEMISTRY
including biophysical chemistry & molecular biology
Article

Steady-State Kinetic and Inhibition Studies of the Mammalian Target of Rapamycin (mTOR) Kinase Domain and mTOR Complexes[†]

Zhihua Tao, John Barker, Stone D.-H. Shi, Michael Gehring, and Shaoxian Sun*

Pfizer La Jolla Laboratories, Worldwide Research and Development, San Diego, California 92121

Received April 30, 2010; Revised Manuscript Received August 30, 2010

ABSTRACT: The mammalian target of rapamycin (mTOR) is a Ser/Thr protein kinase and a major controller of cell growth. In cells, mTOR forms two distinct multiprotein complexes, mTORC1 and mTORC2. The mTORC1 complex can phosphorylate 4EBP1 and S6K1, two key regulators of translation initiation, whereas mTORC2 phosphorylates AKT1, an event required for AKT1 activation. Here, we expressed and purified human mTORC1 and mTORC2 from HEK-293 cells using FLAG-M2 affinity chromatography. Western blotting analysis using phospho-specific antibodies indicated that recombinant mTORC1 and mTORC2 exhibit distinct substrate preferences in vitro, consistent with their roles in cells. To improve our understanding of the enzymatic properties of mTOR alone and mTOR in its complex form, steady-state kinetic profiles of truncated mTOR containing the kinase domain (residues 1360−2549) and mTORC1 were determined. The results revealed that mTORC1 is catalytically less active than truncated mTOR, as evidenced by 4.7- and 3.1-fold decreases in catalytic efficiency, k_{cat}/K_m, for ATP and 4EBP1, respectively. We also found that truncated mTOR undergoes autophosphorylation through an intramolecular mechanism. Mass spectrometric analysis identified two novel mTOR autophosphorylation sites, Ser2454 and either Thr2473 or Thr2474, in addition to the previously reported Ser2481 site. Truncated mTOR and mTORC1 were completely inhibited by ATP competitive inhibitors PI103 and BEZ235 and partially inhibited by rapamycin/FKBP12 in a noncompetitive fashion toward ATP. All inhibitors tested exhibited similar inhibitory potencies between mTORC1 and truncated mTOR containing the kinase domain. Our studies presented here provide the first detailed kinetic studies of a recombinant mTOR complex.

The mammalian target of rapamycin (mTOR)[1] is a member of the phosphoinositide 3-kinase-related kinase (PIKK) family that plays a pivotal role in the regulation of cell growth and has recently been implicated as a potential drug target in the treatment of different types of human cancers (*1*, *2*). It is a large (2549 residues), highly conserved Ser/Thr protein kinase composed of multiple functional domains (*1*). The N-terminus of mTOR (residues 1−1482) contains ~20 tandem HEAT repeats, which are thought to mediate protein−protein interactions. The centrally located FAT domain (residues 1513−1910) is relatively conserved in the PIKK family proteins and may act as a structural scaffold. Immediately downstream of the FAT domain is the FRB domain (residues 2015−2114), to which rapamycin, a specific mTOR inhibitor, binds to form a complex with auxiliary protein FKBP12. Following the FRB domain is a kinase catalytic domain (residues 2181−2484), which is highly homologous to that of phosphatidylinositol 3-kinase (PI3K). The C-terminus of mTOR contains another FAT domain, designated as FATC (residues 2517−2549), reported to be essential for mTOR activity (*3*).

In mammalian cells, mTOR exists in two structurally and functionally distinct protein complexes, mTORC1 and mTORC2. The mTORC1 complex consists of mTOR, Raptor, and mLST8. Raptor associates with mTOR at multiple binding sites and has been proposed to function as a scaffold protein to present substrates to mTORC1 (*4*, *5*). The interaction between mLST8 and the mTOR kinase domain may regulate the stability of mTOR−Raptor association in response to nutrient conditions (*6*). The mTORC1 complex controls protein synthesis via phosphorylation of eIF-4E binding protein 1 (4EBP1) and ribosomal protein S6 kinase 1 (S6K1), two key regulators of mRNA translation and ribosome biogenesis. mTORC1 phosphorylates 4EBP1 at four sites in a hierarchical manner, with phosphorylation of Thr37 and Thr46 preceding that of Ser65 and Thr70 (*7*, *8*). The phosphorylation of S6K1 by mTORC1 occurs on residue Thr389 within the hydrophobic motif of S6K1 (*9*). In cells, mTORC1 is activated by growth factors and insulin via a PI3K-regulated pathway, involving AKT-mediated phosphorylation and inhibition of TCS2 and the subsequent activation of the small GTPase Rheb (*10*). In addition, amino acids also stimulate the activity of mTORC1, and accumulating evidence suggests a key role for Rag GTPase in this event (*11*−*13*). The rapamycin/FKBP12 complex regulates this pathway by acutely inhibiting mTORC1 activity in cells. The inhibition of mTOR by rapamycin is suggested to occur at least in part via dissociation of Raptor from mTOR, which uncouples mTOR from its substrate proteins (*14*).

[†]This work was supported by the Pfizer La Jolla Laboratories Postdoctoral Program.

*To whom correspondence should be addressed: 10646 Science Center Dr., San Diego, CA 92121. Phone: (858) 526-4922. Fax: (858) 526-4240. E-mail: shaoxian.sun@pfizer.com.

[1]Abbreviations: 4EBP1, eukaryotic translation initiation factor 4E-binding protein 1; FAT, FRAP-ATM-TRAPP2; FRB, FKBP12·rapamycin-binding; HEAT, Huntington, elongation factor 3, the A subunit of protein phosphatase 2A, and TOR1; HEK-293, human embryonic kidney 293; Hsp70, heat-shock protein 70; LC−MS/MS, liquid chromatography−tandem mass spectrometry; mTOR, mammalian target of rapamycin; PI3K, phosphatidylinositol 3-kinase; S6K1, ribosomal protein S6 kinase 1; SEC, size-exclusion chromatography; TCA, trichloroacetic acid; TR-FRET, time-resolved fluorescence resonance energy transfer; TSC2, tuberous sclerosis complex 2.

 Published on Web 08/30/2010

The mTORC2 complex consists of multiple proteins, including mTOR, Rictor, Sin1, mLST8, and Protor1. Both Rictor and Sin1 are required for the assembly and function of mTORC2 (*15*). Protor1 binds specifically to Rictor (*16*), and its role in the complex remains elusive. The mTORC2 complex phosphorylates AKT1 at residue Ser473 (*17*), which, along with PDK1-mediated phosphorylation of Thr308, drives full activation of AKT1 (*18*). Also, mTORC2 modulates cytoskeleton organization via regulation of PKC phosphorylation (*19*, *20*). The activity of mTORC2 is insensitive to acute rapamycin treatment; however, prolonged treatment can affect mTORC2 assembly and inhibit AKT1 signaling in certain cell lines through an unknown mechanism (*21*).

Given the importance of mTOR complexes in the regulation of cell growth and proliferation, it is highly desirable to understand the mechanism of function and regulation of the enzyme complex at the molecular level. However, because of the large size and the complexity of the multiple protein components in the mTOR complexes, the purification of recombinant mTOR complexes has not yet been achieved. All previously reported biochemical characterizations used the immune complex obtained from the immunoprecipitation of mTOR and its partners, which does not provide quantitative analysis of mTOR complexes. Consequently, there is a lack of detailed enzyme kinetic parameters of the mTOR complexes in the literature. A truncated form of mTOR containing the kinase domain has been overexpressed and purified from mammalian cells and is often utilized in screening for novel inhibitors (*22*). Careful evaluation of the effects of these inhibitors on mTOR complexes is required to confirm the inhibition and selectivity against mTORC1 and mTORC2. Here, we describe the overexpression of recombinant human mTORC1 and mTORC2 in HEK-293 cells and the purification by anti-FLAG-M2 affinity chromatography. We report the steady-state kinetic parameters of mTORC1 and compared them to those of the truncated form of mTOR (residues 1360−2549) that retains the FAT, FRB, kinase domain, and FATC. Kinase active site inhibitors (PI103 and BEZ235) and an allosteric site inhibitor (rapamycin) (Scheme 1) were tested with both mTORC1 and the truncated mTOR containing the kinase domain. These results provide the first detailed kinetic description and characterization of inhibitors for mTOR complexes. We also report here the identification of two novel mTOR autophosphorylation sites, Ser2454 and either Thr2473 or Thr2474.

MATERIALS AND METHODS

Plasmids, Antibodies, and Other Biochemicals. HA-tagged human mTOR, FLAG-tagged human Raptor, human mLST8, FLAG-tagged mouse Rictor, human Sin1, human Protor1, and GST-tagged human 4EBP1 plasmids were obtained from the Division of Signal Transduction Therapy (University of Dundee, Angus, U.K.). The details of these constructs were previously described (*16*). The gene encoding 4EBP1 was amplified by polymerase chain reaction (PCR) using 4EBP1/pGEX as a template and 5′-GCCCCGGAATTCGCCCATATG-3′ (forward) and 5′-GCTATGCGGCCGCTCGAG-3′ (reverse) primers. The PCR product was digested with *Nde*I and *Xho*I and ligated into the corresponding restriction sites in pET-28b, such that the 4EBP1 produced carried an N-terminal hexahistidine tag (His_6 tag). Truncated mTOR protein (residues 1360−2549) was obtained from Invitrogen. The Western blot antibodies for mTOR, Raptor, mLST8, Rictor, Sin1, and Protor1 were obtained from the Division of Signal Transduction Therapy, University of Dundee. Anti-phospho-4EBP1 (Thr37/46), phospho-S6K1 (Thr389), and phospho-AKT1 (Ser473) antibodies were purchased from Cell Signaling. PI103 and rapamycin were obtained from Calbiochem. BEZ235 was obtained from Selleck. His_6-tagged human FKBP12 protein was purchased from BPS Bioscience Inc. GST-tagged S6K1 (residues 1−421) was purchased from Abcam. [γ-^{33}P]ATP was purchased from PerkinElmer. ATP, trichloroacetic acid (TCA), dimethyl sulfoxide (DMSO), CHAPS, and Tween 20 were obtained from Sigma. All general reagents used for buffers and assays were ACS grade or better.

Scheme 1: Chemical Structures of mTOR Inhibitors PI103, BEZ235, and Rapamycin

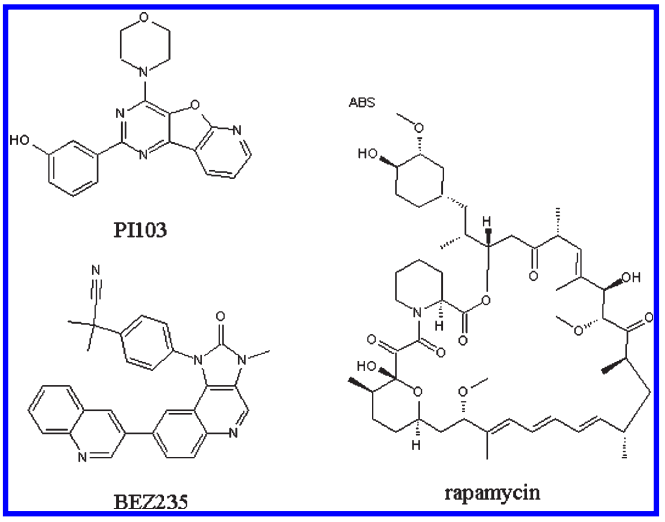

Overexpression and Purification of Human mTORC1 and mTORC2. Recombinant mTORC1 and mTORC2 were overexpressed in HEK-293 cells by using the FreeStyle 293 expression system (Invitrogen) following the manufacturer's instructions. Suspension FreeStyle 293-F cells were maintained in FreeStyle 293 expression medium in shaker flasks at 37 °C with a humidified atmosphere of 8% CO_2. For overexpression of mTORC1, 1 L of cells was transiently cotransfected with 830 μg of HA-mTOR, 430 μg of FLAG-Raptor, and 340 μg of mLST constructs using 1.4 mL of FreeStyle MAX reagent at a cell density of 1.0×10^6 cells/mL. For overexpression of mTORC2, cells were transiently cotransfected with 830 μg of HA-mTOR, 340 μg of FLAG-Rictor, 340 μg of mLST, 240 μg of Sin1, and 150 μg of Protor1 constructs under the same conditions that were used for the production of mTORC1. At 48 h post-transfection, cells were harvested by centrifugation at 1000*g* for 15 min.

The cell pellet was lysed for 20 min in 70 mL of lysis buffer containing 40 mM HEPES (pH 7.5), 120 mM NaCl, 1 mM EDTA, 10 mM sodium pyrophosphate, 10 mM sodium glycerophosphate, 50 mM sodium fluoride, 0.5 mM sodium orthovanadate, 0.2% CHAPS, and protease inhibitors (Roche). Insoluble materials were removed by centrifugation at 20000*g* for 20 min. To purify mTORC1 or mTORC2, 1.5 mL of pre-equilibrated anti-FLAG M2 affinity gel (Sigma) was added to the clear lysate and the mixture was incubated at 4 °C for 1 h with gentle shaking. The gel was then washed with 15 mL of lysis buffer, followed by 15 mL of wash buffer [25 mM HEPES (pH 7.4) and 120 mM NaCl]. The bound mTORC1 or mTORC2 was eluted with 6 mL of 100 μg/mL 3× FLAG peptide (Sigma) in wash buffer, followed by concentration using an Amicon ultra YM-100 centrifugal filter

device (Millipore). The purified mTORC1 and mTORC2 were aliquoted, flash-frozen, and stored at −80 °C.

The protein components in each of the mTOR complexes were confirmed by SDS−PAGE gel and Western blotting analysis. The concentrations of commercially obtained truncated mTOR (Invitrogen), recombinant mTORC1, and mTORC2 were determined on the basis of the intensity of the mTOR protein band on the SDS−PAGE gel in reference to a standard curve of BSA. Briefly, protein samples of truncated mTOR, mTORC1, and mTORC2 along with a series of BSA dilutions with known quantities were loaded on an SDS−PAGE gel. The gel was stained with SYPRO Orange (Invitrogen) and read on a Storm Imager (Molecular Dynamics) in blue fluorescence mode. The intensities of the BSA bands were quantified using ImageQuant (Molecular Dynamics) and were used to generate a standard curve of protein concentration. Protein concentrations were determined on the basis of the intensity of the protein band corresponding to truncated mTOR or mTOR protein in mTOR complexes in comparison to the BSA standard curve. The measured concentration of truncated mTOR was similar to the concentration provided by the vendor. The concentration of mTORC1 was also confirmed by titration of mTORC1 with a tight binding inhibitor BEZ235, which measured the catalytically active mTORC1 concentration. The active site titration revealed that 83% of the purified mTORC1 was able to bind to inhibitor (Figure S1 of the Supporting Information). The protein concentrations determined by protein band intensity on an SDS−PAGE gel were used to calculate the protein specific activity for truncated mTOR and mTOR complexes.

The formation of mTOR complexes was confirmed by molecular mass analysis using TSK-Gel G4000SW (Tosoh Bioscience) analytical size exclusion chromatography (Hitachi D-7000 HPLC system). The column was equilibrated with a running buffer containing 25 mM HEPES (pH 7.4) and 100 mM NaCl. The purified mTOR complexes were eluted with running buffer at a flow rate of 0.7 mL/min for 30 min. The protein peaks were monitored at 280 nm. The retention time corresponding to the molecular mass was calibrated with gel filtration protein standards (Bio-Rad).

Overexpression and Purification of 4EBP1. The 4EBP1/pET-28b plasmid was transformed into *Escherichia coli* BL21-(DE3)pLysS (Invitrogen), and the transformants were selected by kanamycin (50 μg/mL) and chloramphenicol (35 μg/mL). An overnight culture (1 mL each) was used to inoculate 4 L (in 4 × 1 L aliquots) of LB medium containing the selective antibiotics. The cells were grown in LB medium at 37 °C until the OD_{600} reached 0.6. IPTG (final concentration of 0.2 mM) was then added to induce the overexpression of 4EBP1. The cells were allowed to grow at 37 °C for an additional 3 h and then harvested by centrifugation (7000*g* for 10 min).

Cells were resuspended in lysis buffer [25 mM HEPES (pH 7.4), 300 mM NaCl, 10 mM imidazole, and 1 mM β-mercaptoethanol]. Cells were then disrupted by being passed three times through an Y110 microfluidizer (Microfluidics Corp.), followed by centrifugation at 20000*g* for 20 min. The clarified cell lysate was incubated with 10 mL of Ni-NTA resin (Qiagen) in a rotator for 1 h. The resin was collected by centrifugation (800*g* for 5 min), transferred to a 25 mL column, and washed with 100 mL of lysis buffer. The His_6-tagged 4EBP1 was eluted from the column with the HEPES buffer described above containing 0.25 M imidazole. The desired protein fractions were pooled and dialyzed against three changes of 1 L of dialysis buffer [25 mM HEPES (pH 7.4), 120 mM NaCl, and 1 mM β-mercaptoethanol]. The purified His_6-tagged 4EBP1 was flash-frozen in liquid N_2 and stored in aliquots at −80 °C. The concentration of 4EBP1 protein was determined by the Bradford assay (Bio-Rad).

Determination of Substrate Selectivity and Metal Preference of Truncated mTOR and mTOR Complexes by Western Blotting Analysis. Reaction mixtures containing truncated mTOR, mTORC1, or mTORC2 as the kinase and GFP-tagged 4EBP1 (200 nM), GST-tagged S6K1 (200 nM, truncated form, residues 1−421), or GFP-tagged AKT1 (400 nM) as the protein substrate were used in an assay buffer consisting of 50 mM HEPES (pH 7.4), 10 mM $MnCl_2$, 1 mM EGTA, and 0.01% Tween 20. This buffer was used for all the mTOR assays reported in this study unless otherwise noted. Final concentrations of 4 nM for truncated mTOR, 30 nM for mTORC1, and 12 nM for mTORC2 were used in these reactions. Reactions were initiated via the addition of 20 μM ATP, mixtures incubated at room temperature for 20 min, and then reactions quenched via the addition of an equal volume of 2× SDS loading buffer. Phosphorylation of the substrates was detected by Western blotting using phospho-specific antibodies. The control lane shows the reaction mixture without mTOR enzyme, representing the background phosphorylation level of the substrate protein. Enzyme activity was determined by quantification of the band intensity on Western blot membranes using ImageJ. Enzyme activity was then normalized to the concentration of mTOR enzyme used in the reaction and expressed as the percentage of activity of the truncated mTOR.

To study the metal cofactor preference for truncated mTOR, mTORC1, and mTORC2, kinase reactions were performed as described above, but with the variations of metal cofactor in the assay buffer. In these reactions, either 10 mM Mn^{2+}, 5 mM Mn^{2+} and 5 mM Mg^{2+}, or 10 mM Mg^{2+} was used. A control experiment was conducted with 5 mM Mn^{2+} and 5 mM Mg^{2+} in the absence of mTOR enzyme.

Radiometric Filtration Assay. The mTOR activity was determined by measuring the amount of [γ-^{33}P]phosphate from ATP incorporated into the substrate protein. The assays were performed in a volume of 20 μL in low-binding 384-well plates (Costar) at 25 °C. The assay buffer contained 50 mM HEPES (pH 7.4), 10 mM $MnCl_2$, 1 mM EGTA, and 0.01% Tween 20.

To determine the kinetic parameters for ATP turnover, assays contained 14.4 nM truncated mTOR or 29 nM mTORC1, 40 μM His_6-tagged 4EBP1, and various concentrations of ATP mixture (0−250 μM) containing unlabeled ATP and [γ-^{33}P]ATP (400 Ci/mol). To determine the kinetic parameters for 4EBP1 phosphorylation, assays were conducted in the presence of 4 nM truncated mTOR or 6.7 nM mTORC1, a 300 μM ATP mixture containing unlabeled ATP and [γ-^{33}P]ATP (400 Ci/mol), and various concentrations of 4EBP1 (0−90 μM). The reaction was initiated via the addition of the ATP mixture. After incubation at room temperature for 1 h, the reaction was quenched via the addition of 20 μL of chilled 20% TCA. The reaction mixture was then transferred to a 96-well PVDF filtration plate (Millipore) and filtered through a PVDF membrane by vacuum. The PVDF membrane was washed seven times with 100 μL of chilled 20% TCA and dried under vacuum, followed by the addition of 50 μL of a scintillation solution. The plate was sealed and counted in a Packard Topcount NXT scintillation counter. The ^{33}P CPM (counts per minute) was converted into molar terms from the specific activity of the initial ATP stock. The steady-state kinetic parameters were obtained by fitting the initial rates to

the Michaelis−Menten equation (eq 1) using GraphPad Prism version 5.0 (GraphPad Inc.)

$$v_0 = \frac{v_{max}[S]}{K_m + [S]} \quad (1)$$

where v_0 is the initial reaction rate, v_{max} is the maximum reaction rate, [S] is the substrate concentration, and K_m is the substrate concentration at the half-maximal rate.

To determine the potency of inhibitors, reaction mixtures containing 10 nM truncated mTOR or 20 nM mTORC1 and 40 μM His_6-tagged 4EBP1 in assay buffer were incubated with various concentrations of inhibitors [final DMSO concentration of 1% (v/v)] for 10 min before the kinase assay was started via the addition of 100 μM [γ-^{33}P]ATP (1000 Ci/mol). IC_{50} values were determined by fitting the data to eq 2 using GraphPad Prism version 5.0

$$v_i = \frac{v_0 + v_s([I]/IC_{50})}{1 + [I]/IC_{50}} \quad (2)$$

where v_0 and v_i are the reaction rates obtained in the absence and presence of inhibitor, respectively, v_s is the reaction rate at the saturating inhibitor concentration, [I] is the inhibitor concentration, and IC_{50} is the inhibitor concentration that yields the half-maximal inhibition. The K_i value is derived from the IC_{50} based on eq 3 for the competitive inhibitor.

$$K_i = \frac{IC_{50}}{1 + \frac{[S]}{K_m}} \quad (3)$$

For the tight binding inhibitor BEZ235, the data were fit to the Morrison equation (eq 4), and the K_i values were calculated using eq 5.

$$v_i/v_0 = 1 - \frac{[E] + [I] + K_i^{app} - \sqrt{([E]+[I]+K_i^{app})^2 - 4[E][I]}}{2[E]} \quad (4)$$

$$K_i^{app} = K_i\left(1 + \frac{[S]}{K_m}\right) \quad (5)$$

For the mTOR reaction using GFP-AKT1 as a substrate, assay mixtures contained 40 nM truncated mTOR, 800 nM GFP-AKT1, and a 100 μM ATP mixture of unlabeled ATP and [γ-^{33}P]ATP (1000 Ci/mol) in 20 μL of assay buffer. Autophosphorylation of truncated mTOR or AKT1 was assessed under identical conditions except in the absence of GFP-AKT1 or truncated mTOR, respectively. The truncated mTOR-catalyzed phosphorylation of GFP-AKT1 was calculated by subtraction of autophosphorylation of truncated mTOR and GFP-AKT1 from the total phosphorylation.

To investigate the mechanism of mTOR autophosphorylation, the effect of mTOR concentration on the rate of autophosphorylation was evaluated. Reaction mixtures containing various concentrations of truncated mTOR (15, 30, or 60 nM) were incubated with a 20 μM ATP mixture of unlabeled ATP and [γ-^{33}P]ATP (1000 Ci/mol) in 200 μL of assay buffer. The reactions were initiated via the addition of ATP. Aliquots (20 μL) were removed from the reaction mixture at various time points and added to 20 μL of 20 mM EDTA to quench the reactions. At the end of the incubation, 40 μL of chilled 20% TCA was added to the quenched reaction mixtures, and the mixtures were incubated for additional 10 min to allow the proteins to precipitate. The filtration and scintillation counting steps follow the procedures described above. The extent of autophosphorylation was expressed as the number of phosphates incorporated per truncated mTOR molecule.

TR-FRET Assay. The LanthaScreen TR-FRET mTOR assay was performed using Costar low-binding 384-well plates at room temperature according to the instructions of the manufacturer (Invitrogen). The supplied TR-FRET mTOR assay kit contained recombinant, truncated mTOR (residues 1360−2549), GFP-4EBP1, LanthaScreen terbium-labeled anti-phospho-4EBP1 (Thr46), and antibody dilution buffer. To determine the kinetic parameters for ATP turnover, 1 nM truncated mTOR or 3 nM mTORC1 was incubated with 200 nM GFP-4EBP1 and various concentrations of ATP (0−250 μM) in 50 μL of assay buffer. Reactions were initiated via the addition of ATP. Aliquots (10 μL) were taken at five time points (0, 1.5, 3, 4.5, and 6 min) from the incubation mixture, and the reactions were quenched by addition of 10 μL of TR-FRET dilution buffer containing 20 mM EDTA and 4 nM terbium-labeled anti-phospho-4EBP1 (Thr46) detection antibody. After incubation at room temperature for 1 h, the plate was read using a Tecan 2 plate reader with an excitation wavelength of 330 nm (20 nm bandpass) and emission wavelengths of 485 nm (20 nm bandpass), and 515 nm (20 nm bandpass). The TR-FRET ratio for each sample was calculated by dividing the emission signal at 515 nm by the emission signal at 485 nm. The initial reaction velocities were expressed as TR-FRET ratio per minute. The steady-state kinetic parameters were obtained by fitting the initial reaction velocities to the Michaelis−Menten equation (eq 1).

For inhibitor titration experiments, 1 nM truncated mTOR or 3 nM mTORC1 was incubated with 200 nM GFP-4EBP1, 4 μM ATP, and various concentrations of inhibitors in 10 μL of assay buffer. After incubation at room temperature for 15 min, 10 μL of TR-FRET dilution buffer containing 20 mM EDTA and 4 nM terbium-labeled anti-phospho-4EBP1 (Thr46) antibody was added. All the following steps were performed as described above.

For the TR-FRET mTOR assay using GFP-AKT1 as a substrate, the reaction mixtures contained 5 nM truncated mTOR, 800 nM GFP-AKT1, and 20 μM ATP in 10 μL of assay buffer. The same assay procedure described above was performed except that the reaction was allowed to proceed for 1 h and a terbium-labeled anti-phospho-AKT1 (Ser473) antibody was used for detection of the phosphorylated product.

Identification of mTOR Autophosphorylation Sites by LC−MS/MS. To identify the autophosphorylation sites in mTOR, we first subjected truncated mTOR to the in vitro autophosphorylation reaction. Truncated mTOR (1 μM) was mixed with 250 μM ATP in 20 μL of assay buffer. The enzymatic reaction was allowed to proceed at room temperature for 1 h. A control was run under identical conditions except without ATP. The reactions were stopped by the addition of 2× SDS loading buffer, and the mixture was then resolved on a 4 to 12% SDS−PAGE gel. After Coomassie blue staining, the protein band corresponding to truncated mTOR was excised, washed, and incubated with trypsin for in-gel digestion.

The digested peptides from truncated mTOR were analyzed with a capillary LC−MS/MS system consisting of a Thermo LTQ linear ion trap mass spectrometer coupled with an Eksigent NanoLC 2D system through a Michrom ADVANCE CaptiveSpray source. The peptides were separated on a Michrom Halo

0.2 mm × 100 mm capillary column with a 60 min gradient at a flow rate of 1000 nL/min. The acquired data-dependent acquisition LC−MS/MS data were processed on an Agilent SpectrumMill system against Swissprot (version 55.2) or human IPI (version 3.39) databases.

To assess whether the autophosphorylation sites identified from truncated mTOR represent the autophosphoylation sites of mTORC1, a targeted LC−MS^3 method was developed to analyze the in vitro autophosphorylated mTORC1 by use of the parent ion inclusion list function of the data-dependent acquisition on the LTQ. The method targets three m/z values for MS/MS (m/z 861.70 for the peptide containing phosphorylated Ser2454, m/z 924.70 for the peptide containing phosphorylated Thr2473 or Thr2474 and Ser2478 or Ser2481, and m/z 873.90 for the peptide containing phosphorylated Ser1418), as well as three transitions for MS^3 experiments (m/z 861.70−979.50 for y_{18}^{2+}, m/z 924.70−1116.31 for y_{20}^{2+}, and m/z 873.90−655.28 for y_5).

RESULTS

Purification of Recombinant Human mTORC1 and mTORC2. We overexpressed mTORC1 and mTORC2 in HEK-293 cells transiently cotransfected with full-length mTOR, FLAG-Raptor, mLST8 for mTORC1 or full-length mTOR, FLAG-Rictor, mLST8, Sin1, and Protor1 for mTORC2. Recombinant mTORC1 and mTORC2 were purified by anti-FLAG M2 affinity chromatography. The SDS−PAGE gel analysis showed that Raptor and mTOR were the major protein bands for mTORC1 and Rictor and mTOR were the major bands for mTORC2 (Figure 1A,B). Other components of mTOR complexes are also visible on the SDS−PAGE gel at the expected molecular mass, although the staining intensities were much weaker. The presence of these components was also confirmed by trypsin in-gel digestion followed by MS analysis (data not shown). Both mTORC1 and mTORC2 contained a contaminant protein migrating at a molecular mass of approximately 70 kDa (Figure 1A,B). MS analysis identified this band as the heat shock protein Hsp70, a protein known to bind to FLAG resin nonspecifically with high affinity. All the overexpressed protein components in the mTOR complexes were confirmed by Western analysis (Figure 1A,B).

The expected molecular masses of recombinant mTORC1 and mTORC2 are 475 and 620 kDa, respectively. Analytical SEC analysis of recombinant mTORC1 and mTORC2 revealed two protein peaks eluting with the expected retention time (Figure 1C). The protein components for the recombinant mTORC1 and mTORC2 in the elution fraction of these two peaks were confirmed by Western blotting analysis (data not shown). High-molecular mass aggregates were observed for both mTORC1 and mTORC2, with the aggregation of mTORC2 being more severe (Figure 1C). Further evaluation of these aggregates found that they were eluted at the void volume of a TSK gel G4000SW gel filtration column (exclusion limit of 10000 kDa), suggesting a high degree of oligomerization of mTORC1 and mTORC2.

Substrate Selectivity and Metal Preference of Truncated mTOR and mTOR Complexes. The substrate selectivity of recombinant truncated mTOR, mTORC1, and mTORC2 in vitro was investigated using 4EBP1, AKT1, and S6K1 as substrates. As shown in Figure 2A, all three versions of the mTOR enzyme were able to phosphorylate 4EBP1 at Thr37 and Thr46, AKT1 at Ser473, and S6K1 at Thr389; however, their specific activities differed. Truncated mTOR exhibited the highest

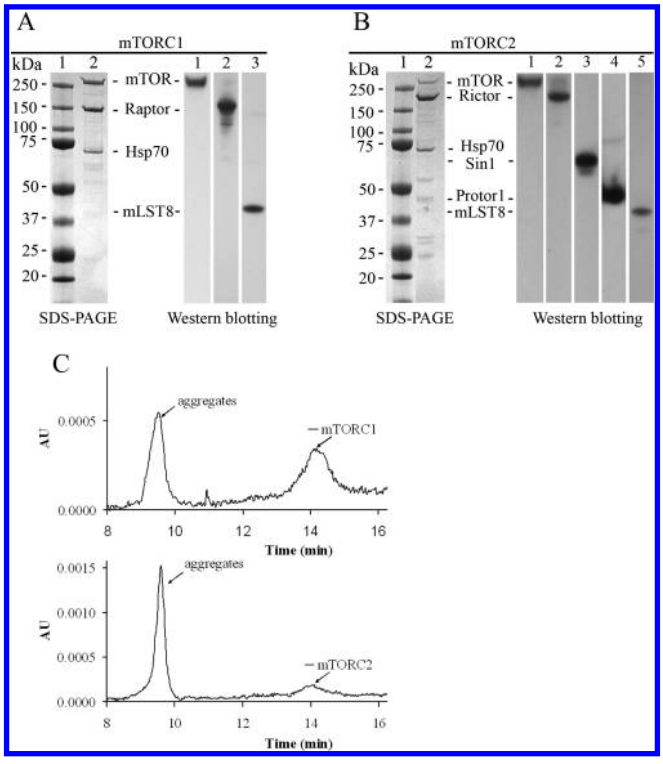

FIGURE 1: Characterization of recombinant human mTORC1 and mTORC2. (A) SDS−PAGE gel showing purified mTORC1 (lane 2) and molecular mass standards (lane 1) (left panel). Western analysis with the appropriate antibodies confirms the presence of mTOR (lane 1), Raptor (lane 2), and mLST8 (lane 3) in purified mTORC1 (right panel). (B) SDS−PAGE gel showing purified mTORC2 (lane 2) and molecular mass standards (lane 1) (left panel). Western blotting analysis with the appropriate antibodies confirms the presences of mTOR (lane 1), Rictor (lane 2), Sin1 (lane 3), Protor1 (lane 4), and mLST8 (lane 5) in purified mTORC2 (right panel). (C) Analytical SEC analysis of purified recombinant mTORC1 and mTORC2. The positions of mTORC1, mTORC2, and aggregates are marked.

activity toward all the tested protein substrates under our reaction conditions (Figure 2A, column chart). Purified mTOR complexes exhibited distinct substrate selectivity, with mTORC1 favoring 4EBP1 as a preferred substrate, whereas mTORC2 was more active toward AKT1. When 4EBP1 was used as a substrate, the activities of mTORC1 and mTORC2 were around 60 and 11% of the activity of truncated mTOR, respectively. With AKT1 as a substrate, mTORC1 and mTORC2 exhibited 11 and 45% of the activity of truncated mTOR, respectively. The substrate selectivity of purified mTOR complexes in vitro is consistent with their substrate selectivity in cells. Although S6K1 is a well-established mTORC1 substrate in cells, our in vitro results demonstrated that both mTORC1 and mTORC2 possessed a comparable activity toward truncated S6K1 (residues 1−421), which is ~4% of that of truncated mTOR.

Previously, it was noted that mTOR itself prefers Mn^{2+} over Mg^{2+} as a metal cofactor for autophosphorylation and phosphorylation of 4EBP1 (*23*). To investigate whether the metal preference of mTOR is altered by the partner proteins and whether it is substrate-dependent, the activities of mTORC1, mTORC2, and truncated mTOR were measured using either 4EBP1 or AKT1 as a substrate in the presence of Mn^{2+}, Mg^{2+}, or both. As shown in Figure 2B, all three forms of mTOR enzymes preferred Mn^{2+} over Mg^{2+} for maximal activity.

Steady-State Kinetics of Truncated mTOR and mTORC1. The steady-state kinetics of truncated mTOR and mTORC1 were

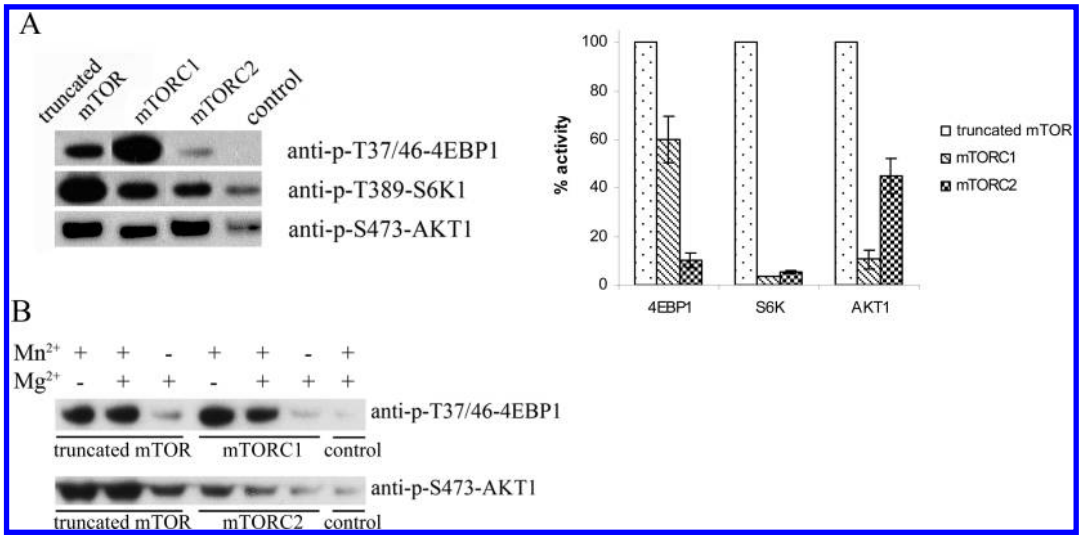

FIGURE 2: Substrate selectivity and metal preference of mTOR complexes and truncated mTOR. (A) Truncated mTOR, mTORC1, and mTORC2 have distinct protein substrate preferences. Phosphorylation of the substrates was detected by Western blotting using phospho-specific antibodies. Final concentrations of 4 nM for truncated mTOR, 30 nM for mTORC1, and 12 nM for mTORC2 were used in these reactions. The control lane shows the reaction mixture without the mTOR enzyme, representing the background phosphorylation level of the substrate protein. The column chart shows quantification of Western blotting (average of the results from two independent experiments). Enzyme activity was normalized to the concentration of enzyme and was expressed as the percentage of the activity of truncated mTOR. (B) Truncated mTOR, mTORC1, and mTORC2 prefer Mn^{2+} to Mg^{2+} as the metal cofactor. Kinase reactions were performed with either 10 mM Mn^{2+}, 5 mM Mn^{2+} and 5 mM Mg^{2+}, or 10 mM Mg^{2+} as the metal cofactor as indicated. A control experiment was conducted with 5 mM Mn^{2+} and 5 mM Mg^{2+} in the absence of mTOR.

Table 1: Steady-State Kinetic Parameters for Truncated mTOR and mTORC1 Determined by a Radiometric Assay

	enzyme	K_m (4EBP1) (μM)	K_m (ATP) (μM)	k_{cat} (min^{-1})	k_{cat}/K_m (4EBP1) (μM^{-1} min^{-1})	k_{cat}/K_m (ATP) (μM^{-1} min^{-1})
4EBP1 phosphorylation	truncated mTOR	6.1 ± 2.0	33 ± 7	0.91 ± 0.13	0.15 ± 0.05	0.028 ± 0.007
	mTORC1	9.5 ± 1.5	74 ± 6	0.47 ± 0.07	0.049 ± 0.010	0.006 ± 0.001

determined using His_6-tagged 4EBP1 and [γ-^{33}P]ATP as substrates by a radiometric filtration assay. This method measured the amount of [^{33}P]phosphate incorporated into the substrate protein. Phosphorylation of 4EBP1 by mTOR occurs at multiple residues; thus, incorporation of ^{33}P into 4EBP1 should provide an index of the total phosphorylation at multiple sites. The steady-state kinetic parameters of mTORC1 and truncated mTOR are summarized in Table 1, and the representative Michaelis−Menten plots are shown in Figure S2A,B of the Supporting Information. It appears that mTORC1 is slightly less active than truncated mTOR, as evidenced by a decreased k_{cat} (0.47 ± 0.07 min^{-1} for mTORC1 vs 0.91 ± 0.13 min^{-1} for truncated mTOR), an increased K_m for ATP (74 ± 6 μM for mTORC1 vs 33 ± 7 μM for truncated mTOR), and a similar K_m for 4EBP1 (9.5 ± 1.5 μM for mTORC1 vs 6.1 ± 2.0 μM for truncated mTOR). As a result, the catalytic efficiency, k_{cat}/K_m, was 4.7-fold decreased for ATP and 3.1-fold decreased for 4EBP1.

The apparent K_m values for ATP were also determined using a TR-FRET assay, which monitors the FRET signal upon binding of phosphorylated GFP-4EBP1 to terbium-labeled anti-phospho-GFP-4EBP1 (Thr46). This assay offers the advantages of higher screening throughput and higher sensitivity, requiring >10-fold less enzyme. The apparent K_m values for ATP were determined to be 3.9 ± 0.4 and 4.1 ± 0.7 μM for truncated mTOR and mTORC1, respectively (Table 2 and Figure S2C of the Supporting Information). These values are 10−20-fold lower than those obtained using the radiometric assay. The discrepancy may be attributed to differences in the assay conditions. In the radiometric filtration assay, the K_m for ATP was determined at a saturating concentration of 40 μM 4EBP1, while in TR-FRET assay, the GFP-4EBP1 concentration was limited to 0.2 μM. Attempts to determine the apparent K_m value for ATP at 0.2 μM 4EBP1 using the radiometric filtration assay were not successful, because of the weak "signal" (phosphorylation of 4EBP1 by truncated mTOR) to "noise" (autophosphorylation of truncated mTOR) ratio under these conditions. His_6-tagged 4EBP1 and GFP-4EBP1 showed no difference in the kinetic parameters determined by the radiometric assay (data not shown).

Autophosphorylation of Truncated mTOR and mTORC1. Previous studies have demonstrated that mTOR is autophosphorylated at Ser2481 in a hydrophobic region near the conserved carboxyl-terminal mTOR tail (*24*). To provide further insight into the mechanism of mTOR autophosphorylation, we monitored the time course for the truncated mTOR autophosphorylation reaction at three enzyme concentrations (15, 30, and 60 nM). The results (Figure 3) showed that the rate of truncated mTOR autophosphorylation is independent of the enzyme concentration, indicating that the reaction occurs by an intramolecular mechanism. The maximal extent of phosphate incorporation, expressed as the number of phosphates incorporated per truncated mTOR molecule, was approximately the same, yielding an average value of 3.7 ± 0.2 phosphates per truncated mTOR molecule. This result indicates mTOR can autophosphorylate at residues other than Ser2481, which is consistent with the previous observation that an mTOR mutant with

Table 2: Steady-State Kinetic Parameters for Truncated mTOR and mTORC1 Determined by the TR-FRET Assay

enzyme	[rapamycin] (nM)	K_m^{app} (ATP) (μM)	k_{cat}^{app} (FRET signal μM^{-1} min^{-1})	k_{cat}^{app}/K_m^{app} (ATP) (FRET signal μM^{-2} min^{-1})
mTORC1	0	3.9 ± 0.4	83 ± 8	26 ± 4
truncated mTOR	0	4.1 ± 0.7	410 ± 15	100 ± 17
truncated mTOR	8	4.4 ± 0.7	300 ± 10	68 ± 11
truncated mTOR	20	5.6 ± 0.8	210 ± 7	38 ± 6
truncated mTOR	128	6.3 ± 1.1	140 ± 6	22 ± 4

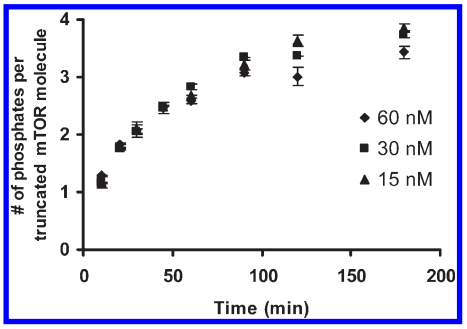

FIGURE 3: Assay time course of truncated mTOR-catalyzed autophosphorylation conducted at three concentrations of truncated mTOR (15, 30, and 60 nM) in the presence of [γ-^{33}P]ATP. The ^{33}P CPM was converted into molar terms according to the specific activity of the ATP stock. The extent of autophosphorylation (y-axis) was expressed as the number of phosphates incorporated per truncated mTOR molecule. At saturation (180 min), an average of 3.7 ± 0.2 phosphates was incorporated into each truncated mTOR molecule.

Ser2481 changed to alanine is still capable of autophosphorylation (*24*).

To identify the remaining autophosphorylation sites, truncated mTOR was incubated in the presence and absence of ATP and analyzed by LC−MS/MS. Two monophosphorylated peptides ($_{1407}$GPTPAILESLISINNK$_{1422}$ and $_{2446}$TDSYSAGQSVEILDGVELGEPAHK$_{2469}$) and one diphosphorylated peptide ($_{2471}$TGTTVPESIHSFIGDGLVKPEALNK$_{2495}$) were observed in the ATP-treated sample (Figure 4 and Figure S3 of the Supporting Information). The phosphorylation sites in the two monophosphorylated peptides were identified as Ser1418 (Figure S3 of the Supporting Information) and Ser2454 (Figure 4, top panel), respectively. However, we were unable to determine unambiguously which of the two sites were phosphorylated in the diphosphorylated peptide (Figure 4, bottom panel), because of the weakness of the ion series and the proximity of Ser and Thr residues within this peptide. Nevertheless, the observed MS/MS fragmentation pattern was consistent with one phosphorylation site localized to either Thr2471, Thr2473, or Thr2474, while the other was either Ser2478 or Ser2481 (Figure 4, bottom panel). The phosphorylation of the mTOR region of residues 2471−2474 has previously been reported in a MS-based kinome study but could not be specifically identified because of a lack of fragmentation (*25*, *26*). Our results were able to localize the autophosphorylation sites because of a stronger signal. We performed MS^3 experiments on the b_5 and $b_5 - H_3PO_4$ ions of the diphosphorylated peptide $_{2471}$TGTTVPESIHSFIGDGLVKPEALNK$_{2495}$. The b_5 ion gave only further loss of H_3PO_4, but MS^3 of $b_5 - H_3PO_4$ gave fragments that ruled out the possibility of the phosphate on Thr2471 (Figure S4 of the Supporting Information). Fragment ions specific to both Thr2473 and Thr2474 were observed, indicating that both residues were phosphorylated (Figure S4 of the Supporting Information). The other phosphorylation site (Ser2478 or Ser2481) detected in the diphosphorylated peptide could be Ser2481, the autophosphorylation residue reported in a previous study (*24*).

In the control sample (non-ATP-treated sample), only one monophosphorylation peptide ($_{1407}$GPTPAILESLISINNK$_{1422}$) was detected. The signal intensity of this phosphopeptide in the control sample was comparable to that in the ATP-treated sample. In addition, the phosphorylation of Ser2454, Thr2473 or -2474, and Ser2478 or -2481, but not Ser1418, was sensitive to the inhibition by BEZ235 (data not shown). Together, these results demonstrate that Ser2454, Thr2473 or -2474, and Ser2478 or -2481 are mTOR autophosphorylation sites in vitro, while Ser1418 was most likely phosphorylated by a separate kinase when expressed in insect cells.

To test whether the autophosphorylation at the specific sites in truncated mTOR also occurs in the mTOR complex, the recombinant mTORC1 was subjected to in vitro autophosphorylation and then digested with trypsin in solution. Because the peptide concentration of digested mTORC1 was low and present in the matrix of many other peptides, initial efforts to detect the phosphopeptides by LC−MS/MS were unsuccessful. We therefore developed a targeted LC−MS^3 method (see Materials and Methods for details) to specifically detect the potential phosphorylation of Ser2454, Thr2473 or -2474, and Ser2478 or -2481 in autophosphorylated mTORC1. These results clearly show that all these three residues were phosphorylated in ATP-treated mTORC1 (Figures S5 and S6 of the Supporting Information). Interestingly, these three sites are also phosphorylated in recombinant mTORC1 without ATP treatment, although the intensities of phosphopeptides were much lower than those detected in the ATP-treated sample. These results suggest that phosphorylation of these residues indeed occurs in cells. We also used the targeted LC−MS^3 method to investigate the phosphorylation state of Ser1418 in both ATP-treated and non-ATP-treated mTORC1. We found that Ser1418 was not phosphorylated in either case.

Inhibition of Truncated mTOR and mTORC1 by ATP Competitive Inhibitors and Rapamycin/FKBP12. The inhibition of truncated mTOR and mTORC1 by small molecules was characterized by both a radiometric filtration assay and a TR-FRET assay (Table 3). The K_i values were consistent between the two methods. PI103 and BEZ235 exhibited nearly complete inhibition of truncated mTOR and mTORC1, while rapamycin, which binds to a unique site in the FRB domain, only partially inhibited truncated mTOR and mTORC1 (Figure 5A,B and Figure S7 of the Supporting Information). In addition, all three compounds showed similar inhibitory potencies toward truncated mTOR and mTORC1, suggesting that the presence of mTOR partner proteins does not affect the binding of these compounds.

To investigate whether rapamycin/FKBP12 inhibition of mTOR activity is substrate-dependent, the effect of rapamycin/

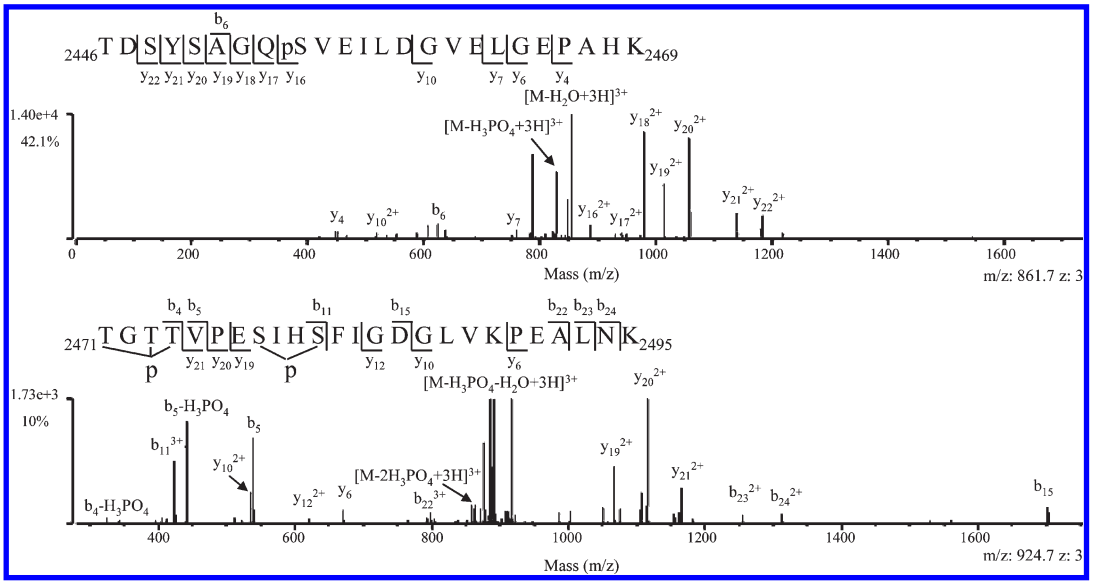

FIGURE 4: Identification of truncated mTOR autophosphorylation sites by LC−MS/MS. MS/MS spectrum showing phosphorylation of Ser2454 (top). MS/MS spectrum showing phosphorylation of Thr2471, -2473, or -2474 and Ser2478 or -2481 (bottom).

Table 3: Inhibitory Potencies of PI103, BEZ235, and Rapamycin against Truncated mTOR and mTORC1

	truncated mTOR			mTORC1		
	PI103	BEZ235	rapamycin	PI103	BEZ235	rapamycin
			Parameters Determined by a Radiometric Assay			
IC_{50} (nM)	82 ± 12	9.6 ± 0.9	9.6 ± 1.0	42 ± 5	8.0 ± 0.8	6.4 ± 1.2
K_i (nM)	20 ± 3	2.5 ± 0.2	not available	18 ± 2	3.2 ± 0.2	not available
			Parameters Determined by a TR-FRET Assay			
IC_{50} (nM)	38 ± 6	3.9 ± 0.2	13 ± 3	42 ± 4	4.2 ± 0.4	13 ± 3
K_i (nM)	19 ± 3	1.7 ± 0.2	not available	21 ± 2	1.5 ± 0.2	not available

FKBP12 on the activity of truncated mTOR was also examined with AKT1 as a substrate. As shown in Figure 5C and Figure S8 of the Supporting Information, both the radiometric assay and the TR-FRET assay demonstrated that phosphorylation of AKT1 by truncated mTOR was also partially inhibited by rapamycin/FKBP12. In addition, rapamycin/FKBP12 also exhibited partial inhibition of the autophosphorylation of truncated mTOR (Figure 5D). Together, these results suggest that rapamycin/FKBP12 might directly inhibit the intrinsic catalytic activity of mTOR in vitro.

The mechanism of rapamycin/FKBP12 inhibition of mTOR was further investigated using the TR-FRET assay with 4EBP1 as a substrate. The Michealis−Menten kinetic analysis was performed in the presence of various concentrations of rapamycin (Figure S9 of the Supporting Information). Within experimental error, the apparent K_m for ATP was unchanged by the addition of rapamycin/FKBP12 (Table 2). The turnover rate, k_{cat}, however, decreased with an increase in rapamycin concentration (Table 2), a pattern that is consistent with noncompetitive inhibition with respect to ATP.

DISCUSSION

Previous biochemical studies using mTOR immune complexes obtained from immunoprecipitation have suggested that binding of Raptor to mTOR is necessary for the mTOR-catalyzed phosphorylation of 4EBP1 (*4*), while the presence of Rictor is required for the mTOR-catalyzed phosphorylation of AKT1 (*17*). Our activity assays using recombinant mTORC1 and mTORC2 demonstrate that although these two mTOR complexes possess a distinct substrate preference, they also exhibit cross reactivity with the protein substrates. It is noteworthy that although S6K1 has long been considered as a mTORC1-specific substrate, our results demonstrate that both recombinant mTORC1 and mTORC2 can phosphorylate Thr389 of truncated S6K1 with comparable efficiency in vitro. This is consistent with a previous study that reported that the structure of S6K1 determines whether mTORC1 or mTORC2 phosphorylate its hydrophobic motif residue, and that phosphorylation of Thr389 of S6K1 by mTORC2 depends on the removal of the carboxyl-terminal domain of S6K1 (*27*). In addition, truncated mTOR alone, without any mTOR partner proteins, is able to phosphorylate both mTORC1-specific substrates, 4EBP1 and S6K1, and the mTORC2-specific substrate, AKT1. In cells, the phosphorylation of each of these mTOR substrates might be contributed by all three forms of mTOR enzyme, free mTOR enzyme, mTORC1, and mTORC2, depending on the relative partitioning of mTOR into these three forms. Determining whether the substrate cross reactivity of mTOR complexes plays a significant role in cellular mTOR signaling under certain circumstances requires further investigation.

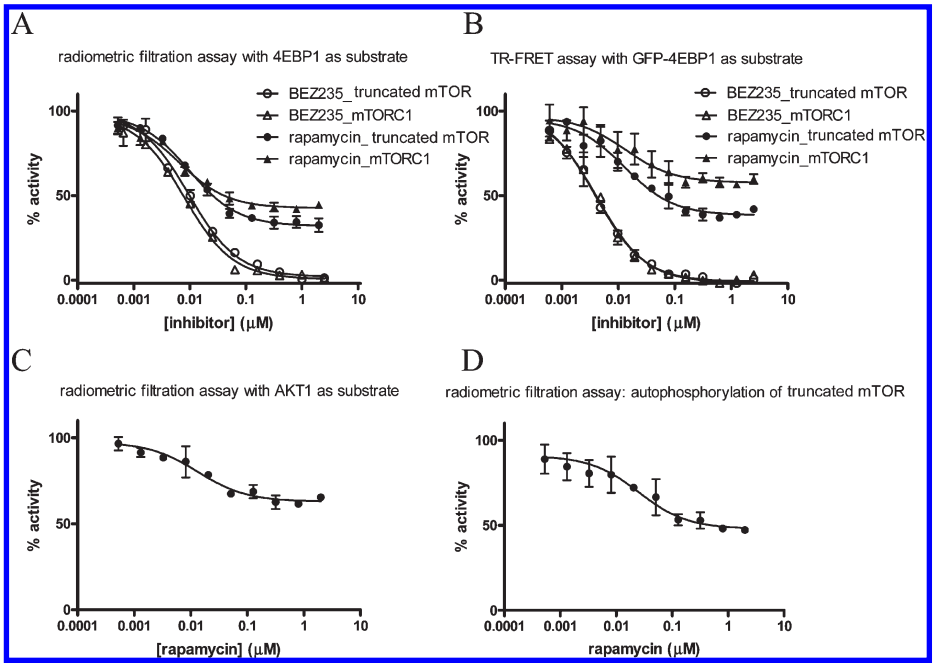

FIGURE 5: Inhibition of truncated mTOR and mTORC1 activities by BEZ235 and rapamycin/FKBP12. The percentage notations reflect the percentage of enzyme activity compared with no inhibitor controls. For rapamycin treatment, 200 nM FKBP12 was also included as an auxiliary protein. (A) Dose−response curves of the effects of inhibitors on the activities of truncated mTOR and mTORC1, as determined using a radiometric filtration assay with 4EBP1 as the protein substrate. (B) Dose−response curves of the effects of inhibitors on the activities of truncated mTOR and mTORC1, as determined using a TR-FRET assay with GFP-4EBP1 as the protein substrate. (C) Dose−response curves of the effects of rapamycin/FKBP12 on the truncated mTOR-catalyzed AKT1 phosphorylation. (D) Dose−response curves of the effects of rapamycin/FKBP12 on truncated mTOR-catalyzed autophosphorylation.

Our detailed kinetic analysis revealed that recombinant mTORC1 exhibited a lower catalytic efficiency toward ATP and 4EBP1 compared to that of truncated mTOR. Because of the low yield and low activity of purified mTORC2, it was not feasible to perform satisfactory kinetic studies of mTORC2 under our reaction conditions, yet we found by Western analysis that truncated mTOR was also more active than mTORC2 toward AKT1 phosphorylation. Several factors could account for the lower activity of recombinant mTORC1 compared to that of truncated mTOR. One possibility is that N-terminal HEAT repeats of mTOR, postulated to be involved in protein−protein recognition with mTOR partner proteins, could interact with the kinase domain in the context of full-length molecules so that it might repress mTOR catalytic activity. Indeed, previous studies by Western analysis have suggested that truncated mTOR is slightly more active than full-length mTOR (*22*). Alternatively, Raptor could have a negative regulatory role for mTOR activity. This is supported by the finding that a strong association between mTOR and Raptor actually leads to inhibition of mTOR catalytic activity (*5*). Taken together, we propose that it is possible that the mTOR complex with multiple proteins assembled together achieves substrate selectivity at the cost of catalytic activity.

Our results show that the ATP K_m values for truncated mTOR and mTORC1 were 33 ± 7 and 74 ± 6 μM, respectively. These values are close to the result (50 μM) generated by Toral-Barza et al. (*22*) but are significantly lower than the K_m value (> 1 mM) estimated by Western blotting analysis by Dennis et al. (*28*). Both the report by Toral-Barza et al. and our studies utilized Mn^{2+} as the metal cofactor in the mTOR assays, while Dennis et al. used Mg^{2+} in their assays. We also tested Mg^{2+} in our assays. However, because both truncated mTOR and mTOR complexes have much lower activity toward MgATP than MnATP (Figure 2B), we were not able to determine the K_m for MgATP with either the TR-FRET assay or the radiometric filtration assay because of the low signal to noise ratio. Determining whether the discrepancies in the reported ATP K_m values for mTOR are caused by the utilization of different metal cofactors requires further investigation.

Truncated mTOR is commonly used in the screening of inhibitors because of its commerical availability. The question of whether the inhibitor potency measured with the truncated mTOR remains the same against mTOR complexes arises. Our studies showed that the K_i values for all three inhibitors tested were in excellent agreement between truncated mTOR and mTORC1, suggesting a similar sensitivity of truncated mTOR and mTORC1 to the inhibition by small molecules, albeit with different substrate selectivities.

It was previously hypothesized that rapamycin inhibits mTORC1 through a mechanism in which Raptor is dissociated from mTOR, affecting the binding of substrate to mTOR (*5*, *14*). However, a study by Jacinto et al. (*29*) showed that Raptor copurified with mTOR on immobilized FKBP12 in the presence of rapamycin, implying rapamycin does not cause the dissociation of the complex. Studies by Soliman et al. (*30*) agree well with those of Jacinto et al. in showing that rapamycin reduces the level of mTORC1-associated mTOR autophosphorylation, a read-out of mTORC1 intrinsic catalytic activity. During the revision of this work, Yip et al. (*31*) reported a cryo-EM structure of human TORC1 and proposed that binding of rapamycin to mTORC1 disintegrated the dimeric mTORC1 complex in a stepwise manner, leading to a time-dependent inhibition of 4EBP1. They also suggested that the binding of rapamycin to mTORC1 might block the access of a large-sized substrate S6K1 to the active site; therefore, a rapid inhibition of phosphorylation of S6K1 by rapamycin was observed. Our data demonstrate that rapamycin

inhibits truncated mTOR-catalyzed phosphorylation of 4EBP1 and AKT1 as well as autophosphorylation of truncated mTOR, suggesting that rapamycin might directly inhibit the catalytic activity of the mTOR enzyme. This inhibition by rapamycin was partial and noncompetitive against ATP, consistent with recent reports that rapamycin is only a partial antagonist of mTORC1 in cells (*32*, *33*). Interestingly, the concentrations of rapamycin that were effective in inhibiting mTOR kinase activity in our biochemical studies (IC_{50} = 10 nM) were higher than those in blocking mTOR function in cells (IC_{50} = 1 nM) (*34*−*36*). In cells, additional factors could contribute to the inhibitory effects of rapamycin on mTOR function in addition to the direct inhibition of the catalytic activity. For instance, rapamycin may inhibit mTOR substrate phosphorylation by activation of PP2A phosphatase (*37*). Alternatively, the potent inhibitory effect of rapamycin in cells may arise from the blockage of mTOR activation by phosphatidic acid (PA) binding (*38*), which is supported by the solution structure of the FRB−PA complex where the residues interacting with PA closely match the sites responsible for rapamycin binding (*39*).

Autophosphorylation is a salient feature shared by many protein kinases and may represent an important mechanism in the modulation of kinase activities as well as their cellular functions (*40*). Previously, it was reported that mTOR catalyzes autophosphorylation both in vitro and in vivo, and the autophosphorylated residue was identified as Ser2481, a site near the conserved carboxyl-terminal tail (*24*, *30*). In our study, two novel autophosphorylation sites, Ser2454 and either Thr2473 or Thr2474, were found to be phosphorylated in truncated mTOR in the presence of ATP, but not in the absence of ATP, suggesting that these modifications are a result of autophosphorylation. These two residues were also phosphorylated in recombinant mTORC1 produced from mammalian cells, consistent with recent MS-based kinome studies (*25*, *26*, *41*). The phosphorylation of these two residues in cells could be a result of autophosphorylation or could be performed by another kinase. Nevertheless, our MS studies indicate the intensities of phosphopeptides are much higher in ATP-treated mTORC1 than those in non-ATP-treated mTORC1, providing supporting evidence that these two residues could be autophosphorylated by mTORC1 as well. Interestingly, Thr2473 or Thr2474 is in the proximity of the previously identified autophosphorylation residue Ser2481, and Ser2454 is near a region that plays an important role in mTOR activity regulation. Deletion of this region leads to elevated mTOR activity both in vitro and in cells (*42*, *43*). In the vicinity of Ser2454, phosphorylation of Thr2446 and Ser2448, mediated by AMPK (*44*) and S6K1 (*45*), respectively, is regulated by nutrient status and growth factors. It remains to be determined whether phosphorylation of Ser2454 and Thr2473 or Thr2474 is regulated by hormones and growth factors, and whether this event plays a regulatory role in mTOR action. Nevertheless, no initial lag phase was observed in the time course of the truncated mTOR-catalyzed reaction, suggesting that autophosphorylation of mTOR might not play a role in activating its enzyme catalytic activity. Another interesting observation is that Ser1418, a residue within the FAT domain of mTOR, is phosphorylated in recombinant truncated mTOR overexpressed in insect cells, but not in recombinant mTORC1 overexpressed in HEK-293 cells. The question of whether the partner proteins in mTORC1 protect the recognition of this residue by the kinase or phosphorylation of this residue is of any physiological significance needs further investigation.

In summary, this study sought to provide an improved understanding of the biochemical properties of the mTOR enzyme and its complexes. We have demonstrated that recombinant mTORC1, mTORC2, and truncated mTOR possess cross reactivity toward different protein substrates along with distinct protein selectivity and similar metal preference for Mn^{2+} over Mg^{2+}. We found that compared to truncated mTOR, recombinant mTORC1 had reduced catalytic activity because of both weaker ATP binding affinity and lower k_{cat} values. The presence of mTOR partners does not affect the sensitivities of mTOR for the ATP competitive inhibitors, PI103 and BEZ235, or the allosteric inhibitor rapamycin. In addition, we identified two novel mTOR autophosphorylation sites, Ser2454 and either Thr2473 or Thr2474, by MS analysis. The significance of the novel autophosphorylation sites in the regulation of mTOR function remains to be investigated.

ACKNOWLEDGMENT

We thank Darryl Nousome and Tom Carlson for their expert technical assistance, Stephan Grant for support and insightful discussion, and Alessi Dario for helpful advice.

SUPPORTING INFORMATION AVAILABLE

Figures showing determination of the mTORC1 concentration using BEZ235, steady-state kinetics of truncated mTOR and mTORC1, MS spectra, the dose−response curve of PI103, and effects of rapamycin on GFP-AKT1 phosphorylation. This material is available free of charge via the Internet at http://pubs.acs.org.

REFERENCES

1. Chiang, G. G., and Abraham, R. T. (2007) Targeting the mTOR signaling network in cancer. *Trends Mol. Med. 13*, 433–442.
2. Guertin, D. A., and Sabatini, D. M. (2007) Defining the role of mTOR in cancer. *Cancer Cell 12*, 9–22.
3. Takahashi, T., Hara, K., Inoue, H., Kawa, Y., Tokunaga, C., Hidayat, S., Yoshino, K., Kuroda, Y., and Yonezawa, K. (2000) Carboxyl-terminal region conserved among phosphoinositide-kinase-related kinases is indispensable for mTOR function in vivo and in vitro. *Genes Cells 5*, 765–775.
4. Hara, K., Maruki, Y., Long, X., Yoshino, K., Oshiro, N., Hidayat, S., Tokunaga, C., Avruch, J., and Yonezawa, K. (2002) Raptor, a binding partner of target of rapamycin (TOR), mediates TOR action. *Cell 110*, 177–189.
5. Kim, D. H., Sarbassov, D. D., Ali, S. M., King, J. E., Latek, R. R., Erdjument-Bromage, H., Tempst, P., and Sabatini, D. M. (2002) mTOR interacts with raptor to form a nutrient-sensitive complex that signals to the cell growth machinery. *Cell 110*, 163–175.
6. Kim, D. H., Sarbassov, D. D., Ali, S. M., Latek, R. R., Guntur, K. V., Erdjument-Bromage, H., Tempst, P., and Sabatini, D. M. (2003) GβL, a positive regulator of the rapamycin-sensitive pathway required for the nutrient-sensitive interaction between raptor and mTOR. *Mol. Cell 11*, 895–904.
7. Gingras, A. C., Gygi, S. P., Raught, B., Polakiewicz, R. D., Abraham, R. T., Hoekstra, M. F., Aebersold, R., and Sonenberg, N. (1999) Regulation of 4E-BP1 phosphorylation: A novel two-step mechanism. *Genes Dev. 13*, 1422–1437.
8. McMahon, L. P., Choi, K. M., Lin, T. A., Abraham, R. T., and Lawrence, J. C., Jr. (2002) The rapamycin-binding domain governs substrate selectivity by the mammalian target of rapamycin. *Mol. Cell. Biol. 22*, 7428–7438.
9. Burnett, P. E., Barrow, R. K., Cohen, N. A., Snyder, S. H., and Sabatini, D. M. (1998) RAFT1 phosphorylation of the translational regulators p70 S6 kinase and 4E-BP1. *Proc. Natl. Acad. Sci. U.S.A. 95*, 1432–1437.
10. Li, Y., Corradetti, M. N., Inoki, K., and Guan, K. L. (2004) TSC2: Filling the GAP in the mTOR signaling pathway. *Trends Biochem. Sci. 29*, 32–38.
11. Sancak, Y., Peterson, T. R., Shaul, Y. D., Lindquist, R. A., Thoreen, C. C., Bar-Peled, L., and Sabatini, D. M. (2008) The Rag GTPases

bind raptor and mediate amino acid signaling to mTORC1. *Science 320*, 1496–1501.
12. Kim, E., Goraksha-Hicks, P., Li, L., Neufeld, T. P., and Guan, K. L. (2008) Regulation of TORC1 by Rag GTPases in nutrient response. *Nat. Cell Biol. 10*, 935–945.
13. Sancak, Y., Bar-Peled, L., Zoncu, R., Markhard, A. L., Nada, S., and Sabatini, D. M. (2010) Ragulator-Rag complex targets mTORC1 to the lysosomal surface and is necessary for its activation by amino acids. *Cell 141*, 290–303.
14. Oshiro, N., Yoshino, K., Hidayat, S., Tokunaga, C., Hara, K., Eguchi, S., Avruch, J., and Yonezawa, K. (2004) Dissociation of raptor from mTOR is a mechanism of rapamycin-induced inhibition of mTOR function. *Genes Cells 9*, 359–366.
15. Yang, Q., Inoki, K., Ikenoue, T., and Guan, K. L. (2006) Identification of Sin1 as an essential TORC2 component required for complex formation and kinase activity. *Genes Dev. 20*, 2820–2832.
16. Pearce, L. R., Huang, X., Boudeau, J., Pawlowski, R., Wullschleger, S., Deak, M., Ibrahim, A. F., Gourlay, R., Magnuson, M. A., and Alessi, D. R. (2007) Identification of Protor as a novel Rictor-binding component of mTOR complex-2. *Biochem. J. 405*, 513–522.
17. Sarbassov, D. D., Guertin, D. A., Ali, S. M., and Sabatini, D. M. (2005) Phosphorylation and regulation of Akt/PKB by the rictor-mTOR complex. *Science 307*, 1098–1101.
18. Alessi, D. R., Andjelkovic, M., Caudwell, B., Cron, P., Morrice, N., Cohen, P., and Hemmings, B. A. (1996) Mechanism of activation of protein kinase B by insulin and IGF-1. *EMBO J. 15*, 6541–6551.
19. Facchinetti, V., Ouyang, W., Wei, H., Soto, N., Lazorchak, A., Gould, C., Lowry, C., Newton, A. C., Mao, Y., Miao, R. Q., Sessa, W. C., Qin, J., Zhang, P., Su, B., and Jacinto, E. (2008) The mammalian target of rapamycin complex 2 controls folding and stability of Akt and protein kinase C. *EMBO J. 27*, 1932–1943.
20. Ikenoue, T., Inoki, K., Yang, Q., Zhou, X., and Guan, K. L. (2008) Essential function of TORC2 in PKC and Akt turn motif phosphorylation, maturation and signalling. *EMBO J. 27*, 1919–1931.
21. Sarbassov, D. D., Ali, S. M., Sengupta, S., Sheen, J. H., Hsu, P. P., Bagley, A. F., Markhard, A. L., and Sabatini, D. M. (2006) Prolonged rapamycin treatment inhibits mTORC2 assembly and Akt/PKB. *Mol. Cell 22*, 159–168.
22. Toral-Barza, L., Zhang, W. G., Lamison, C., Larocque, J., Gibbons, J., and Yu, K. (2005) Characterization of the cloned full-length and a truncated human target of rapamycin: Activity, specificity, and enzyme inhibition as studied by a high capacity assay. *Biochem. Biophys. Res. Commun. 332*, 304–310.
23. Heesom, K. J., and Denton, R. M. (1999) Dissociation of the eukaryotic initiation factor-4E/4E-BP1 complex involves phosphorylation of 4E-BP1 by an mTOR-associated kinase. *FEBS Lett. 457*, 489–493.
24. Peterson, R. T., Beal, P. A., Comb, M. J., and Schreiber, S. L. (2000) FKBP12-Rapamycin-associated Protein (FRAP) Autophosphorylates at Serine 2481 under Translationally Repressive Conditions. *J. Biol. Chem. 275*, 7416–7423.
25. Gnad, F., Ren, S., Cox, J., Olsen, J. V., Macek, B., Oroshi, M., and Mann, M. (2007) PHOSIDA (phosphorylation site database): Management, structural and evolutionary investigation, and prediction of phosphosites. *Genome Biol. 8*, R250.
26. Oppermann, F. S., Gnad, F., Olsen, J. V., Hornberger, R., Greff, Z., Keri, G., Mann, M., and Daub, H. (2009) Large-scale proteomics analysis of the human kinome. *Mol. Cell. Proteomics 8*, 1751–1764.
27. Ali, S. M., and Sabatini, D. M. (2005) Structure of S6 kinase 1 determines whether raptor-mTOR or rictor-mTOR phosphorylates its hydrophobic motif site. *J. Biol. Chem. 280*, 19445–19448.
28. Dennis, P. B., Jaeschke, A., Saitoh, M., Fowler, B., Kozma, S. C., and Thomas, G. (2001) Mammalian TOR: A homeostatic ATP sensor. *Science 294*, 1102–1105.
29. Jacinto, E., Loewith, R., Schmidt, A., Lin, S., Ruegg, M. A., Hall, A., and Hall, M. N. (2004) Mammalian TOR complex 2 controls the actin cytoskeleton and is rapamycin insensitive. *Nat. Cell Biol. 6*, 1122–1128.
30. Soliman, G. A., Acosta-Jaquez, H. A., Dunlop, E. A., Ekim, B., Maj, N. E., Tee, A. R., and Fingar, D. C. (2010) mTOR Ser-2481 autophosphorylation monitors mTORC-specific catalytic activity and clarifies rapamycin mechanism of action. *J. Biol. Chem. 285*, 7866–7879.
31. Yip, C. K., Murata, K., Walz, T., Sabatini, D. M., and Kang, S. A. (2010) Structure of the human mTOR complex I and its implications for rapamycin inhibition. *Mol. Cell 38*, 768–774.
32. Thoreen, C. C., Kang, S. A., Chang, J. W., Liu, Q., Zhang, J., Gao, Y., Reichling, L. J., Sim, T., Sabatini, D. M., and Gray, N. S. (2009) An ATP-competitive mammalian target of rapamycin inhibitor reveals rapamycin-resistant functions of mTORC1. *J. Biol. Chem. 284*, 8023–8032.
33. Feldman, M. E., Apsel, B., Uotila, A., Loewith, R., Knight, Z. A., Ruggero, D., and Shokat, K. M. (2009) Active-site inhibitors of mTOR target rapamycin-resistant outputs of mTORC1 and mTORC2. *PLoS Biol. 7*, e38.
34. Yu, K., Toral-Barza, L., Discafani, C., Zhang, W. G., Skotnicki, J., Frost, P., and Gibbons, J. J. (2001) mTOR, a novel target in breast cancer: The effect of CCI-779, an mTOR inhibitor, in preclinical models of breast cancer. *Endocr.-Relat. Cancer 8*, 249–258.
35. Chen, Y., Zheng, Y., and Foster, D. A. (2003) Phospholipase D confers rapamycin resistance in human breast cancer cells. *Oncogene 22*, 3937–3942.
36. Kuo, C. J., Chung, J., Fiorentino, D. F., Flanagan, W. M., Blenis, J., and Crabtree, G. R. (1992) Rapamycin selectively inhibits interleukin-2 activation of p70 S6 kinase. *Nature 358*, 70–73.
37. Peterson, R. T., Desai, B. N., Hardwick, J. S., and Schreiber, S. L. (1999) Protein phosphatase 2A interacts with the 70-kDa S6 kinase and is activated by inhibition of FKBP12-rapamycinassociated protein. *Proc. Natl. Acad. Sci. U.S.A. 96*, 4438–4442.
38. Fang, Y., Vilella-Bach, M., Bachmann, R., Flanigan, A., and Chen, J. (2001) Phosphatidic acid-mediated mitogenic activation of mTOR signaling. *Science 294*, 1942–1945.
39. Veverka, V., Crabbe, T., Bird, I., Lennie, G., Muskett, F. W., Taylor, R. J., and Carr, M. D. (2008) Structural characterization of the interaction of mTOR with phosphatidic acid and a novel class of inhibitor: Compelling evidence for a central role of the FRB domain in small molecule-mediated regulation of mTOR. *Oncogene 27*, 585–595.
40. Smith, J. A., Francis, S. H., and Corbin, J. D. (1993) Autophosphorylation: A salient feature of protein kinases. *Mol. Cell. Biochem. 127−128*, 51–70.
41. Brill, L. M., Xiong, W., Lee, K. B., Ficarro, S. B., Crain, A., Xu, Y., Terskikh, A., Snyder, E. Y., and Ding, S. (2009) Phosphoproteomic analysis of human embryonic stem cells. *Cell Stem Cell 5*, 204–213.
42. Edinger, A. L., and Thompson, C. B. (2004) An activated mTOR mutant supports growth factor-independent, nutrient-dependent cell survival. *Oncogene 23*, 5654–5663.
43. Sekulic, A., Hudson, C. C., Homme, J. L., Yin, P., Otterness, D. M., Karnitz, L. M., and Abraham, R. T. (2000) A direct linkage between the phosphoinositide 3-kinase-AKT signaling pathway and the mammalian target of rapamycin in mitogen-stimulated and transformed cells. *Cancer Res. 60*, 3504–3513.
44. Cheng, S. W., Fryer, L. G., Carling, D., and Shepherd, P. R. (2004) Thr2446 is a novel mammalian target of rapamycin (mTOR) phosphorylation site regulated by nutrient status. *J. Biol. Chem. 279*, 15719–15722.
45. Chiang, G. G., and Abraham, R. T. (2005) Phosphorylation of mammalian target of rapamycin (mTOR) at Ser-2448 is mediated by p70S6 kinase. *J. Biol. Chem. 280*, 25485–25490.